

Band structure and cohesive properties of 3d-transition-metal carbides and nitrides with the NaCl-type structure

J. Häglund and G. Grimvall

Department of Theoretical Physics, The Royal Institute of Technology, S-100 44 Stockholm, Sweden

T. Jarlborg

Département de Physique de la Matière Condensée, 24, Quai Ernest-Ansermet, CH-1211 Genève 4, Switzerland

A. Fernández Guillermé

Consejo Nacional de Investigaciones Científicas y Técnicas, Centro Atómico Bariloche, 8400 San Carlos de Bariloche, Argentina

(Received 29 November 1990)

We study the cohesive energy of NaCl-structure MX compounds with $X=C$ and N and $M=Sc$, Ti , V , Cr , Mn , Fe , Co , and Ni , by combining *ab initio* total-energy calculations with an analysis of thermodynamic information. Using the linear muffin tin orbital method, we calculate the cohesive energy (E_{coh}) of carbides and nitrides and establish trends as a function of the average number of valence electrons per atom in the compound (n_e). These results are compared with values derived by us from thermodynamic information. Since most of the compounds considered here are metastable, we apply interpolation and extrapolation procedures to get information on their E_{coh} . This allows us to extend the comparison between theory and thermodynamic data to a wider range of n_e values than covered in previous work. We find a remarkable agreement between theoretical and experimental trends. There is, however, a systematic difference between linear muffin tin orbital and thermodynamic values comparable to that observed in calculations for the pure 3d transition metals. The general variation of the cohesive energy is discussed and interpreted in the light of our band-structure results. A more detailed study is carried out for CrN and the NaCl-structure carbide and nitride of Mn .

I. INTRODUCTION

The relation between the cohesive properties of transition-metal compounds and their electronic structure is a matter of considerable theoretical and practical interest. In particular, the properties of MX compounds ($M=3d$ transition metal, $X=C$ and N) with the NaCl structure have been studied theoretically using various methods.¹⁻⁵ Recently, Zhukov *et al.*² calculated the band-structure and cohesive properties of TiC , VC , TiN , and VN using the linear muffin-tin orbital (LMTO) method, and reported a correlation between the cohesive energy (E_{coh}) and the average number of valence electrons per atom (n_e) of the compound. A recent analysis⁶ of experimental data on 3d-transition-metal carbides and nitrides also revealed striking regularities in the variation of cohesive properties with n_e . This was given a qualitative explanation in terms of the filling of bonding and antibonding electron states⁶ in a rigid-band model, relying on the band structure of the NaCl-structure carbides and nitrides of Ti and V .^{1,2}

Most of the band-structure calculations reported previously have been devoted to carbides and nitrides that are stable and hence can be studied experimentally. In order to establish the systematics of bonding properties, it would be useful to consider a larger group of substances, extending to a wide range of n_e . Such a study has been hampered by the lack of reliable experimental informa-

tion on some stable compounds (e.g., of Sc), and by the fact that the NaCl structure becomes metastable in the $M-C$ and $M-N$ phase diagrams for the 3d transition metals placed to the right in the Periodic Table.

It is the purpose of the present work to study the cohesive properties of MX compounds with the NaCl structure, when $X=C$ and N and $M=Sc$, Ti , V , Cr , Mn , Fe , Co , and Ni . Using the LMTO method we calculate their cohesive energy (E_{coh}), and establish trends as a function of the average number of valence electrons per atom (n_e). The theoretical cohesive energies are compared with E_{coh} for stable compounds derived from thermochemical measurements, and with indirect information on metastable compounds obtained from interpolation and extrapolation procedures developed in recent studies.⁶⁻⁹ This allows us to examine the relation between theory and experiments beyond the range of n_e values covered in previous works.

II. CALCULATION OF ELECTRONIC STRUCTURES

A. Method

The electronic structures were calculated using the self-consistent linear muffin-tin orbital method (LMTO).¹⁰ The potential was of local-density type with the parametrization of Gunnarsson and Lundqvist. Relativistic effects were included except for the spin-orbit

coupling for valence electrons. A more detailed description of our LMTO technique can be found elsewhere.¹¹

All carbides and nitrides in this paper were investigated in the NaCl structure containing two atoms per unit cell. The calculations were performed for a 505 k -point mesh in the irreducible wedge of the Brillouin zone. The basis set was chosen to contain s , p , d , and f for the metal atoms and s , p , and d for the carbon and nitrogen atoms. The lattice constants were set equal to the experimental values for the stable compounds (ScC to VC, ScN to CrN) while the lattice constants for the metastable compounds were estimated by performing interpolations and extrapolations in plots of the average volume per atom in the compound (Ω) versus the average number of valence electrons (n_e),^{6,7} cf. Table I. Although these lattice constants do not minimize the total energy, they can be used to obtain reliable cohesive energies, since energy differences corresponding to small variations in the lattice spacing are negligible compared to the energy scales of interest for the conclusions of this paper. The Wigner-Seitz radii were set equal to $0.341a$ for the M atoms and to $0.271a$ for the C and N atoms for all compounds (a is the lattice constant).

In order to obtain as reliable cohesive energies as possible within the local spin-density approximation, a new computer program for the calculation of atomic total energies was developed. We there use exactly the same approximations and the same numerical routines as in the band-structure program. The core levels are treated relativistically while the valence levels deliberately are calculated in a semirelativistic approximation. In the atomic case, the region of low charge density far from the nucleus is accounted for by extending the logarithmic 277-point radial mesh in the bulk program to a 323-point mesh in the atomic program. The calculations of the total energies in both cases are identical except for the Madelung contribution which is not present in the atomic case. We expect that the above precautions lead to significant cancellations of numerical and model-dependent errors between the bulk and atomic calculations and therefore improve the reliability of the obtained cohesive energies. However, the well-known property of the local spin-density approximation to overestimate the cohesive energy in the 3d series¹² is still expected. The total atomic energies for all atoms (except the rare gases) with $Z \leq 53$ are listed, for future reference, in Table II. The electronic configurations in the table are those that minimize the total energies. The fact that they differ significantly from the experimental configurations is known from previous calculations of the same type.¹³ One should note that we, like Moruzzi, Janak, and Williams,¹³ find that a nonintegral configuration minimizes the total atomic energy in two cases: Fe and Co.

B. Results

The calculated band structure of FeC in certain symmetry directions is shown in Fig. 1 as an example of the electronic structure in the 3d carbides and nitrides. The corresponding density of states (DOS) curve is presented in Fig. 2 together with s , p , and d projections summed

over both atoms. The lowest-lying band in these curves can be described as a carbon s band. The region just above the band gap contains mostly hybridized p bands from carbon and d bands from iron. The density of states at the Fermi level is clearly dominated by the d states from iron.

In Fig. 3 the density of states of FeC is plotted versus the average integrated valence charge. The Fermi level of FeC ($n_e = 6e/a$) falls in a distinct minimum in the middle of the d region. Since the density of states of the other carbides and nitrides in the 3d series are quite similar to that of FeC, we can use Fig. 3 to understand why the Fermi level of ScC ($n_e = 3.5$) lies slightly below a deep minimum and why the Fermi levels of TiC and ScN ($n_e = 4$) fall at the bottom of this minimum. Both VC and TiN ($n_e = 4.5$) and CrC and VN ($n_e = 5$) have Fermi levels on the slope of a sharp d peak, while MnC and CrN ($n_e = 5.5$), in their paramagnetic states, have Fermi levels on the top of this peak. The Fermi levels of MnN ($n_e = 6$), CoC, FeN ($n_e = 6.5$), NiC, CoN ($n_e = 7$), and NiN ($n_e = 7.5$) all lie in the upper part of the d region. In three compounds (MnC, MnN, and FeN), we find a ferromagnetic spin splitting of the ground state.

The results of our calculations are summarized in Table I.¹⁴ The cohesive energy per atom is defined by

$$E_{\text{coh}} = -\left(\frac{1}{2}\right)(E_{MX} - E_M - E_X), \quad (1)$$

where E_{MX} is the total electronic energy of the compound MX and E_A ($A = M, X$) are the total atomic energies of the constituent atoms as listed in Table II.

III. COHESIVE ENERGY FROM EXPERIMENTAL INFORMATION

A. Definitions and thermodynamic relations

The experimental analog of the quantity E_{coh} defined in Eq. (1) is the enthalpy change per atom for the reaction



at zero Kelvin and one atmosphere, corrected for the energy of zero-point vibrations in MX , viz.,

$$E_{\text{coh}} \equiv -\left\{\frac{1}{2}\left[{}^0H_{MX}^{\text{st}}(0) - {}^0H_M^{\text{g}}(0) - {}^0H_X^{\text{g}}(0)\right] - \frac{9}{8}k_B\Theta_{MX}\right\}. \quad (3)$$

${}^0H_i^{\text{st}}(0)$ and ${}^0H_i^{\text{g}}(0)$ represent the enthalpy at zero Kelvin and one atmosphere per atom of the substance i ($i = MX, M, X$) in its stable (st) modification and in the gaseous (g) monatomic state, respectively, and Θ_{MX} is a Debye temperature defined so that $\frac{9}{8}k_B\Theta_{MX}$ gives the zero-point vibrational energy per atom of MX . The evaluation of E_{coh} was made by expressing the sum in brackets in Eq. (3) in terms of quantities that are given in standard compilations of thermodynamic data, or have been

TABLE I. Summary of our band-structure calculations on MX carbides and nitrides. The lattice parameters are those that are used in the theoretical calculation. The last column shows the cohesive energies we obtain from thermodynamic information, with our estimate of the probable uncertainties. E_{coh} values in parentheses are based on estimates and interpolations, see Sec. III B.

Compound	n_e (e/a)	Lattice parameter (a.u.)	$N(E_F)$ (states/Ry)	μ_M (μ_B)	μ_X (μ_B)	Charge M (e)	Charge X (e)	Total energy (Ry)	E_{coh} theoretical (mRy/a)	E_{coh} experimental (mRy/a)
SeC	3.5	8.92 ^a	19.9			2.71	4.29	-1600.896	594	468 (± 5)
TiC	4.0	8.18 ^b	3.2			3.79	4.21	-1779.978	672	526 (± 5)
VC	4.5	7.88 ^b	15.8			4.90	4.10	-1970.736	641	510 (± 6)
CrC	5.0	(7.78) ^c	33.3			6.00	4.00	-2173.572	547	(426) (± 9)
MnC	5.5	(7.78) ^d	19.4	1.31	-0.11	7.12	3.88	-2388.885	538	(378) (± 10)
FeC	6.0	(7.72) ^d	9.5			8.19	3.81	-2616.941	575	(417) (± 10)
CoC	6.5	(7.65) ^e	28.2			9.26	3.74	-2858.063	576	(418) (± 10)
NiC	7.0	(7.54) ^e	15.8			10.28	3.72	-3112.522	528	(415) (± 10)
SeN	4.0	8.52 ^a	0.0			2.48	5.52	-1634.333	629	(494) (± 10)
TiN	4.5	8.01 ^b	10.9			3.62	5.38	-1813.282	640	492 (± 5)
VN	5.0	7.83 ^b	24.1			4.71	5.29	-2003.983	580	459 (± 5)
CrN	5.5	7.84 ^a	61.0			5.78	5.21	-2206.781	467	378 (± 6)
MnN	6.0	(7.94) ^f	16.8	3.03	0.14	6.79	5.21	-2422.101	463	(300) (± 20)
FeN	6.5	(7.81) ^g	36.6	2.15	0.18	7.89	5.11	-2650.125	483	(337) (± 6)
CoN	7.0	(7.75) ^h	29.3			9.00	5.00	-2891.236	479	(333) (± 10)
NiN	7.5	(7.75) ⁱ	19.6			10.02	4.98	-3145.714	440	(329) (± 10)

^aExperimental, from Ref. 33.

^bExperimental, quoted in Ref. 2.

^cEstimated value, from Ref. 6. The experimental value $a_0 = 6.84$ a.u. quoted, e.g., in Ref. 4 is too low and probably corresponds to another Cr carbide, cf. our discussion in Ref. 6.

^dEstimated value, from Ref. 6.

^eEstimated value, from Ref. 7.

^fSmooth extrapolation of lattice-parameter data in Ref. 34 for the face-centered tetragonal phases η and Θ of the Mn-N system. The early value $a_0 = 8.38$ a.u. reported for "MnN" from experiments in Ref. 35 is inconsistent with the present extrapolation, and probably too large.

^gEstimated value. Obtained in Ref. 28 by interpolation in a plot of the average volume per atom (Ω) vs n_e for 3d metal nitrides.

^hEstimated value from Ref. 34. Reference 36 gives $a_0 = 8.07$ a.u. for a cubic CoN compound with the NaCl structure, prepared by decomposing $\text{Co}(\text{NH}_2)_3$. A very close value ($a_0 = 8.09$ a.u.) is presented in Ref. 37 for a cubic CoN compound prepared by decomposing $[\text{Co}(\text{NH}_3)_6](\text{N}_3)_3$, but it corresponds to the ZnS structure.

ⁱEstimated value from Ref. 8.

TABLE II. Atomic total energies. The valence configuration is that which minimizes the total energy.

Atom	Configuration	Total energy (Ry)	Atom	Configuration	Total energy (Ry)
H	1s ↑	-0.974	Cu	(3d ↑) ⁵ 4s ↑(3d ↓) ⁵	-3304.750
Li	2s ↑	-14.713	Zn	(3d ↑) ⁵ 4s ↑(3d ↓) ⁵ 4s ↓	-3586.876
Be	2s ↑2s ↓	-28.921	Ga	4s ↑4p ↑4s ↓	-3882.524
B	2s ↑2p ↑2s ↓	-48.537	Ge	4s ↑(4p ↑) ² 4s ↓	-4192.156
C	2s ↑(2p ↑) ² 2s ↓	-75.004	As	4s ↑(4p ↑) ³ 4s ↓	-4515.976
N	2s ↑(2p ↑) ³ 2s ↓	-108.372	Se	4s ↑(4p ↑) ³ 4s ↓4p ↓	-4854.036
O	2s ↑(2p ↑) ³ 2s ↓2p ↓	-149.199	Br	4s ↑(4p ↑) ³ 4s ↓(4p ↓) ²	-5206.714
F	2s ↑(2p ↑) ³ 2s ↓(2p ↓) ²	-198.448	Rb	5s ↑	-5955.943
Na	3s ↑	-323.380	Sr	5s ↑5s ↓	-6352.369
Mg	3s ↑3s ↓	-398.964	Y	4d ↑5s ↑5s ↓	-6763.638
Al	3s ↑3p ↑3s ↓	-483.602	Zr	(4d ↑) ³ 5s ↑	-7190.228
Si	3s ↑(3p ↑) ² 3s ↓	-577.758	Nb	(4d ↑) ⁴ 5s ↑	-7632.443
P	3s ↑(3p ↑) ³ 3s ↓	-681.770	Mo	(4d ↑) ⁵ 5s ↑	-8090.462
S	3s ↑(3p ↑) ³ 3s ↓3p ↓	-795.791	Tc	(4d ↑) ⁵ 5s ↑4d ↓	-8564.290
Cl	3s ↑(3p ↑) ³ 3s ↓(3p ↓) ²	-920.322	Ru	(4d ↑) ⁵ 5s ↑(4d ↓) ²	-9054.406
K	4s ↑	-1201.217	Rh	(4d ↑) ⁵ 5s ↑(4d ↓) ³	-9561.035
Ca	4s ↑4s ↓	-1357.474	Pd	(4d ↑) ⁵ (4d ↓) ⁵	-10084.503
Ca	(3d ↑) ² 4s ↑	-1524.703	Ag	(4d ↑) ⁵ 5s ↑(4d ↓) ⁵	-10624.834
Ti	(3d ↑) ³ 4s ↑	-1703.630	Cd	(4d ↑) ⁵ 5s ↑(4d ↓) ⁵ 5s ↓	-11182.126
V	(3d ↑) ⁴ 4s ↑	-1894.451	In	5s ↑5p ↑5s ↓	-11756.210
Cr	(3d ↑) ⁵ 4s ↑	-2097.475	Sn	5s ↑(5p ↑) ² 5s ↓	-12347.524
Mn	(3d ↑) ⁵ 4s ↑4s ↓	-2312.804	Sb	5s ↑(5p ↑) ³ 5s ↓	-12956.271
Fe	(3d ↑) ⁵ 4s ↑(3d ↓) ^{1.29} (4s ↓) ^{0.71}	-2540.787	Te	5s ↑(5p ↑) ³ 5s ↓5p ↓	-13582.528
Co	(3d ↑) ⁵ 4s ↑(3d ↓) ^{2.73} (4s ↓) ^{0.27}	-2781.907	I	5s ↑(5p ↑) ³ 5s ↓(5p ↓) ²	-14226.632
Ni	(3d ↑) ⁵ 4s ↑(3d ↓) ⁴	-3036.462			

estimated. We write

$$E_{\text{coh}} = -\left(\frac{1}{2}\{\Delta^0 H_{MX}^{\text{st}}(T_0) - \Delta H_0^{T_0}\} - [\Delta^0 H_M^{\text{st} \rightarrow g}(0) + \Delta^0 H_X^{\text{st} \rightarrow g}(0)]\right) - \frac{9}{8} k_B \Theta_{MX}, \quad (4)$$

where

$$\Delta^0 H_{MX}^{\text{st}}(T_0) \equiv {}^0 H_{MX}^{\text{st}}(T_0) - {}^0 H_M^{\text{st}}(T_0) - {}^0 H_X^{\text{st}}(T_0) \quad (5)$$

is the enthalpy of formation of the compound MX from the elements in their stable modifications at one atmosphere and $T_0 = 298.15$ K. This quantity is available from direct measurements in stable compounds and has recently been estimated for the metastable compounds considered in the present work, see below. The term $\Delta H_0^{T_0}$ is defined as

$$\Delta H_0^{T_0} \equiv [{}^0 H_{MX}^{\text{st}}(T_0) - {}^0 H_{MX}^{\text{st}}(0)] - [{}^0 H_M^{\text{st}}(T_0) - {}^0 H_M^{\text{st}}(0)] - [{}^0 H_X^{\text{st}}(T_0) - {}^0 H_X^{\text{st}}(0)] \quad (6)$$

and accounts for the enthalpy difference between temperatures 0 and T_0 . It can be taken directly from thermodynamic measurements for the elements M and X (Refs. 15–18) and for stable MX compounds. The ${}^0 H_{MX}^{\text{st}}(T_0) - {}^0 H_{MX}^{\text{st}}(0)$ term for metastable compounds was expressed as

$${}^0 H_{MX}^{\text{st}}(T_0) - {}^0 H_{MX}^{\text{st}}(0) = \int_0^{T_0} (C_P)_{MX}^{\text{st}} dT \quad (7)$$

and the heat capacity at constant pressure $(C_P)_{MX}^{\text{st}}$ was approximated by using a Debye model with an estimated Θ_{MX} (see below) and neglecting nonvibrational and anharmonic contributions. The terms $\Delta^0 H_M^{\text{st} \rightarrow g}(0)$ and

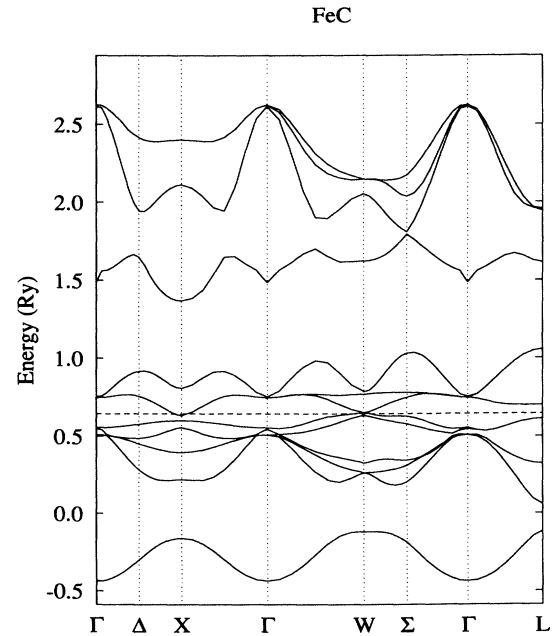


FIG. 1. Electronic band structure of FeC in the NaCl structure in certain symmetry directions.

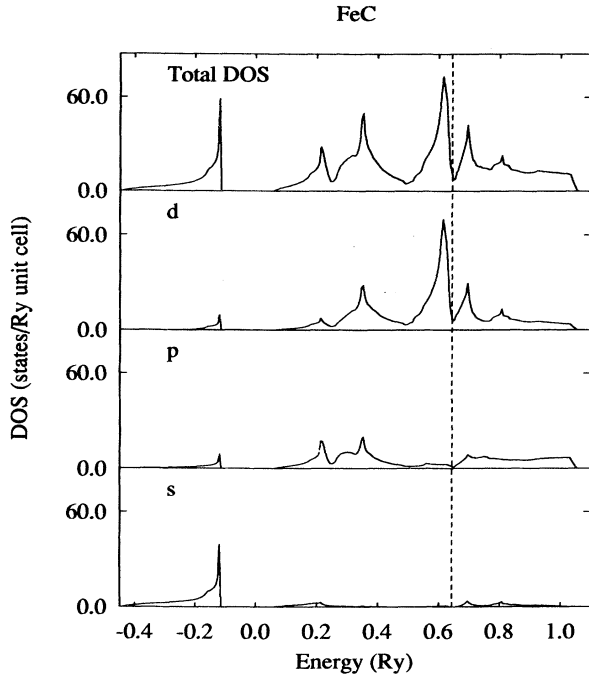


FIG. 2. Electronic density of states of FeC as a function of energy.

$\Delta^0 H_X^{\text{st} \rightarrow \text{g}}(0)$, defined as

$$\Delta^0 H_M^{\text{st} \rightarrow \text{g}}(0) \equiv {}^0 H_M^{\text{g}}(0) - {}^0 H_M^{\text{st}}(0), \quad (8)$$

$$\Delta^0 H_X^{\text{st} \rightarrow \text{g}}(0) \equiv {}^0 H_X^{\text{g}}(0) - {}^0 H_X^{\text{st}}(0), \quad (9)$$

represent the atomization enthalpies of the elements M and X at zero Kelvin and one atmosphere. They are available from compilations of thermodynamic data^{16,17,19,20} for the elements.

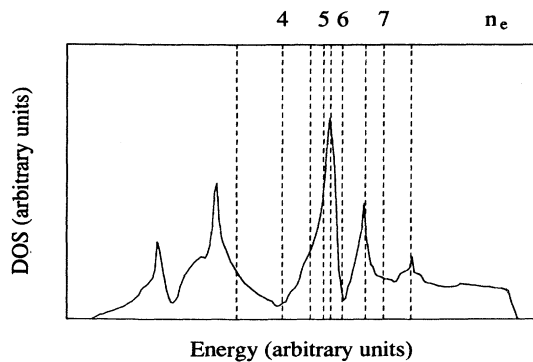


FIG. 3. The dotted lines indicate at which positions of the DOS curve the average integrated valence charge (n_e) takes the values 3.5, 4.0, 4.5, 5.0, 5.5, 6.0, 6.5, 7.0, and 7.5 electrons per atom.

B. Evaluation of E_{coh} for stable and metastable NaCl-structure compounds

The NaCl-structure carbides ScC, TiC, and VC are stable, and their $\Delta^0 H_{MC}^{\text{st}}(T_0)$ are known from experiments.^{16,21,22} Θ_{MX} and ${}^0 H_{MX}^{\text{st}}(T_0) - {}^0 H_{MX}^{\text{st}}(0)$ are known from direct measurements only for TiC (Refs. 16 and 23) and VC.^{24,25} The ${}^0 H_M^{\text{st}}(T_0) - {}^0 H_M^{\text{st}}(0)$ term for ScC was evaluated from Eq. (7) using a Debye temperature obtained by approximating $\Theta_{\text{ScC}} \approx \Theta_{\text{ScC}}^S$, where Θ^S represents the “entropy Debye temperature,”²⁶ which has been evaluated⁶ from high-temperature entropy data. That Θ was also used to evaluate the energy of zero-point vibrations in Eq. (5). The properties of the metastable carbides CrC, MnC, FeC, CoC, and NiC are not known from direct measurements, but their $\Delta^0 H_{MC}^{\text{st}}(T_0)$ and Θ_{MC}^S have been estimated elsewhere⁷ using various interpolation and extrapolation procedures. These results were relied upon in the present work.

ScN, TiN, VN, and CrN are stable nitrides and $\Delta^0 H_{MN}^{\text{st}}(T_0)$ is known from experiments for $M=\text{Ti}, \text{V},$ and Cr .¹⁶ The enthalpy of formation of ScN has not been measured and we used an estimate.⁶ Θ_{MN} for $M=\text{Ti}, \text{V}$ is also available from experiments,^{23,25} while for $M=\text{Sc}, \text{Cr}$ we estimated $\Theta_{MN} \approx \Theta_{MN}^S$, using known entropy Debye temperatures.⁶ The remaining NaCl-structure nitrides of the 3d-transition-metal series are not stable, and we only have indirect information on their properties. Their Θ_{MN}^S were estimated by using interpolation procedures based on the smooth variation of cohesive properties with the average number of valence electrons per atom (n_e) in the compound.⁶ Those results were used to estimate the Debye temperature Θ_{MN} in Eq. (3) as $\Theta_{MN} \approx \Theta_{MN}^S$ ($M=\text{Mn}, \text{Fe}, \text{Co},$ and Ni) and to evaluate ${}^0 H_{MX}^{\text{st}}(T_0) - {}^0 H_{MX}^{\text{st}}(0)$ from Eq. (7). The enthalpy of formation of the metastable NaCl-structure NiN has been obtained⁸ from a thermodynamic analysis of the Ni-N phase diagram based on the “two-sublattice” model for the Gibbs energy of interstitial phases.²⁷ A similar method was later used²⁸ to evaluate $\Delta^0 H^{\text{st}}(T_0)$ for metastable FeN in the NaCl structure, whereas the enthalpy of formation of metastable CoN was obtained here by interpolation in a $\Delta^0 H_{MN}^{\text{st}}(T_0)$ vs n_e plot. Those $\Delta^0 H_{MN}^{\text{st}}(T_0)$ values ($M=\text{Fe}, \text{Co},$ and Ni) were used to evaluate E_{coh} using Eq. (4), whereas E_{coh} for the metastable MnN in the NaCl structure was determined by a smooth interpolation in a E_{coh} vs n_e plot. All cohesive energies obtained in the present work are given in Table I, together with our estimate of their probable uncertainty. E_{coh} obtained by us using estimates and interpolations are given in parentheses.

IV. DISCUSSION

A. Systematics of cohesive properties

In Figs. 4, 5, and 6 we plot theoretical and experimental values of E_{coh} for MX ($X=\text{C}$ and N) compounds versus the position of M in the Periodic Table, and the average number of valence electrons per atom. We use n_e in order to carry out a qualitative discussion in terms of

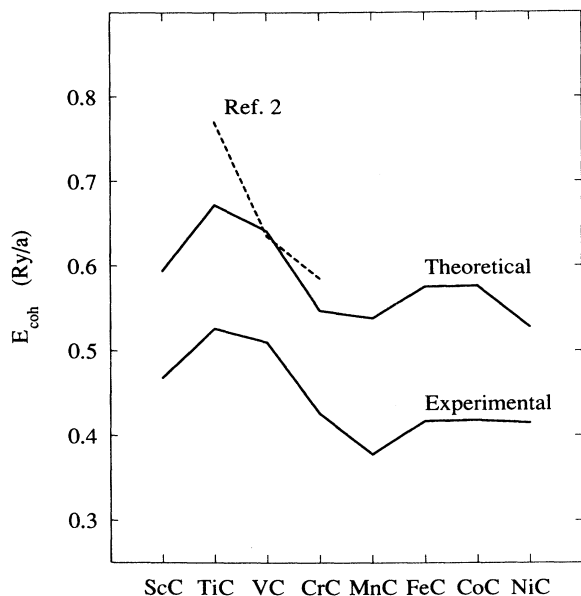


FIG. 4. The cohesive energy (E_{coh}) of the MC carbides. The solid lines show the theoretical and experimental values from this work while the dashed line is from Zhukov *et al.* (Refs. 2 and 4).

band-filling arguments, without regard to the s , p , and d character of the electrons. Calculations and experiments agree on the qualitative features of the E_{coh} vs n_e plot of MC compounds. The largest E_{coh} value is obtained for TiC ($n_e = 4e/a$), which corresponds to the case where the Fermi level falls in deep minimum in the density of states (cf. Fig. 3). When moving from TiC to ScC ($n_e = 3.5e/a$)

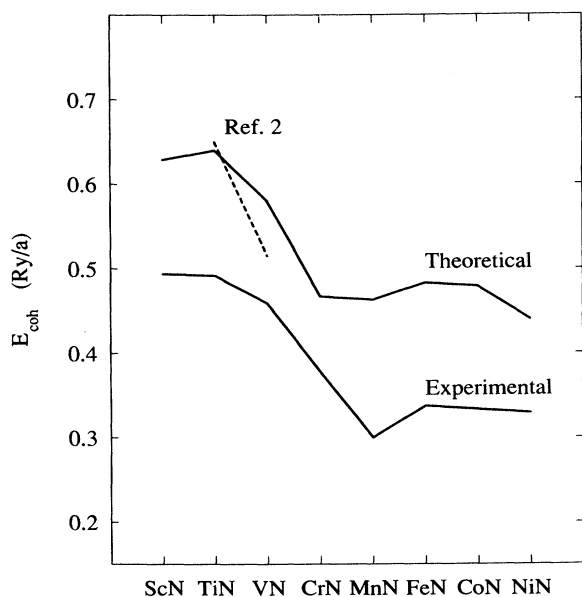


FIG. 5. The cohesive energy (E_{coh}) of the MN carbides. The solid lines show the theoretical and experimental values from this work while the dashed line is from Zhukov *et al.* (Ref. 2).

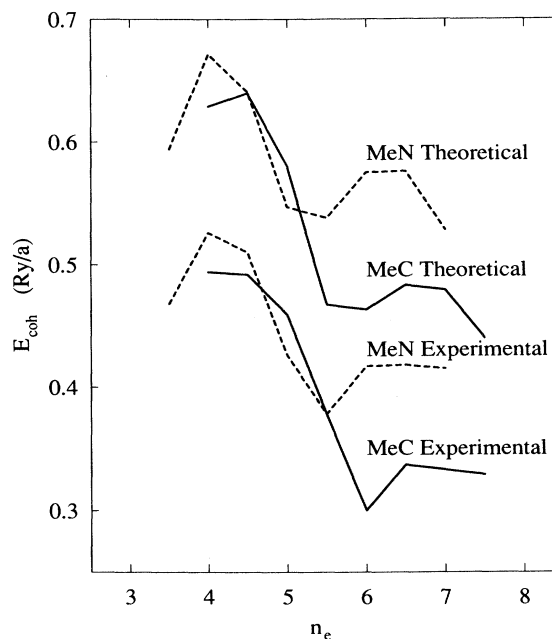


FIG. 6. The cohesive energy per atom (E_{coh}) of the MX carbides and nitrides plotted vs the average number of valence electrons per atom (n_e). The solid lines are our theoretical values from LMTO calculations while the dashed lines show values from our analysis of experimental information.

the theoretical E_{coh} decreases, and so does the experimental value obtained by us from the high-temperature enthalpy of formation.²¹ A previous analysis of entropy data⁶ also indicated that the cohesive energy of ScC would be smaller than that of TiC. When MC changes in the sequence TiC ($n_e = 4e/a$) \rightarrow VC ($n_e = 4.5e/a$) \rightarrow CrC ($n_e = 5e/a$) the Fermi level moves from a deep minimum in the density of states into a region of high density of states (Fig. 3), and E_{coh} decreases. In the range $4e/a \leq n_e \leq 5e/a$, carbides and nitrides with the NaCl structure have similar values of cohesive energy, a regularity that was noted in the LMTO results of Zhukov *et al.*² and in an analysis of vibrational entropy data.⁶ This regularity has previously⁷ been referred to as "homology." When n_e increases beyond $n_e = 5e/a$, both theory and experiments in the present study show that the homology disappears, and the E_{coh} vs n_e relation is split into two slowly varying curves, one for carbides and one for nitrides.

In order to understand why the E_{coh} values for carbides and nitrides are separated above a certain n_e , we have to study the differences in the electronic structure between the two series of compounds. From Table I, we see that the lattice constants are smaller for the carbides than for the corresponding nitrides. The d -band occupation is slightly larger in the carbides which means that, at the respective Fermi energies (E_F), the d functions have smaller amplitudes at the Wigner-Seitz radii (R_{WS}), despite the smaller lattice constants. It then seems reasonable to assume that the carbide lattices can shrink due to more localized $M d$ electrons, i.e., the C atoms

play a more important role in determining the lattice spacing in the carbides than the N atoms do in the nitrides. This can be explained by the fact that the pressure from localized $M d$ electrons is smaller than from delocalized d electrons because of the small amplitudes of the wave functions at R_{WS} . Adding more d electrons to an almost filled band of localized d functions does not lead to further expansion (cf. the smaller lattice constants for larger d occupation in Table I). Therefore, despite the average isoelectronic conditions in MX carbides and nitrides, the former have more $M d$ electrons and thus can shrink more. This additional contraction may be the origin of the lower total energy in the solid phase, which in turn leads to larger cohesive energies for these compounds. It should be noted that these arguments also hold for lower d -band occupations since the carbides always have more $M d$ electrons than the nitrides. However, the difference is that at low d -band filling, the d functions are delocalized with high amplitudes at the Wigner-Seitz radii, and thus the lattice spacing is not so sensitive to the d -band occupation as it is at larger n_e values.

B. LMTO versus experimental results

A significant feature of the results in Fig. 6 is the almost constant difference between calculated and experimental E_{coh} values, which amounts to $140 (\pm 20)$ mRy/atom for carbides and (130 ± 20) mRy/atom for nitrides. The fact that band-structure calculations based on the local-density approximation tend to overestimate E_{coh} for the $3d$ -transition metal elements has been noted before. For instance, Bagno, Jepsen, and Gunnarsson¹² give differences between theory and experiments of the order of 200 mRy/atom, which is comparable with those obtained here.

Our results and those of Zhukov *et al.*² agree on the fact that E_{coh} for MC and MN compounds decreases when M changes from Ti to V. Zhukov *et al.*² analyzed experimental information and concluded that $E_{coh}(\text{TiC}) < E_{coh}(\text{VC})$, in clear disagreement with the theoretical trend. However, it has been noted⁶ that other quantities obtained from experiments change in the same way as the theoretical cohesive energies, and so do the E_{coh} values presented in an earlier²⁹ analysis of experimental data. E_{coh} obtained by us from thermodynamic information (Table I) also supports the theoretical trend. We note that the decrease in E_{coh} of MX ($X=C$ and N) from $M=\text{Ti}$ to $M=\text{V}$ is smaller in our results than according to Zhukov *et al.*² The difference may be due to the fact that Zhukov *et al.* use the "frozen-core" approximation in their calculations while we perform a "free-core" treatment, both in the bulk and in the atomic calculations.

C. Cohesive energy of CrN

Lacking experimental information on the NaCl-structure MC carbides with $n_e > 5e/a$, Fernández Guillermet and Grimvall⁷ assumed that homology relations hold up to $n_e = 5.5e/a$, and a $\Delta^0 H^{st}(T_0)$ value for the

metastable MnC ($n_e = 5.5e/a$) was estimated from the measured properties of CrN ($n_e = 5.5e/a$) as $E_{coh}(\text{MnC}) \approx E_{coh}(\text{CrN})$. Contrasting with this, the LMTO results in Fig. 6 give, at $n_e = 5.5e/a$, $E_{coh}(\text{MnC}) - E_{coh}(\text{CrN}) \approx 70$ mRy/atom, which is larger than the theoretical differences corresponding to the range of n_e (Ref. 6) where homology relations have been observed. Hence our LMTO results suggest that the assumption of homology underestimates the difference in E_{coh} between MnC and CrN. In view of this, we discuss CrN in some detail (see also Fig. 7). Note that our theoretical $E_{coh}(\text{CrN})$ is only 90 mRy/atom larger than the experimental value, whereas the average systematic difference between theory and experiments for the MN compounds is (130 ± 20) mRy/atom. Thus the theoretical E_{coh} for CrN seems to be $130 - 90 = (40 \pm 20)$ mRy/atom smaller than expected from the systematic shift observed for the $3d$ metal MN nitrides. One possible reason why the cohesive energy of CrN could have been underestimated here is that the total energy has been calculated for paramagnetic CrN in the NaCl structure. Experiments, however, refer to antiferromagnetic CrN in which the structure is slightly different from the NaCl type and can be described by an orthorhombic unit cell.³⁰ It cannot be taken for certain that this effect can account for the full difference between the expected and calculated cohesive energies, but waiting for this possibility to be tested by calculation, it is interesting to examine the consequences of a larger $E_{coh}(\text{CrN})$ value on the qualitative features of Fig. 6. For instance, an increase in $E_{coh}(\text{CrN})$ by (40 ± 20) mRy/atom would bring CrN in line with the results for

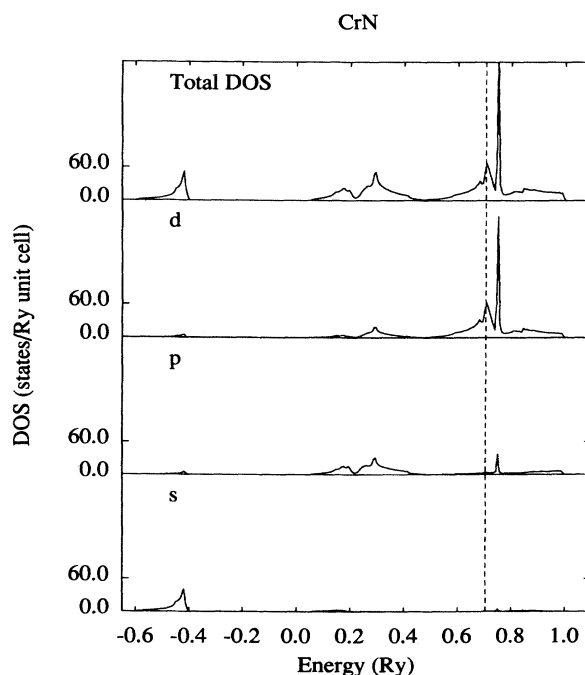


FIG. 7. Electronic density of states of CrN as a function of energy.

the remaining MN nitrides, and would decrease the theoretical difference $E_{\text{coh}}(\text{MnC}) - E_{\text{coh}}(\text{CrN})$ from 70 mRy/atom (see above) to (30 ± 20) mRy/atom. That smaller difference is comparable to the magnitude of those found theoretically between carbides and nitrides with $4e/a \leq n_e \leq 5e/a$, viz. $E_{\text{coh}}(\text{TiC}) - E_{\text{coh}}(\text{ScN}) \approx 43$ mRy/atom, $E_{\text{coh}}(\text{VC}) - E_{\text{coh}}(\text{TiN}) \approx 1$ mRy/atom, and $E_{\text{coh}}(\text{VN}) - E_{\text{coh}}(\text{CrC}) \approx -33$ mRy/atom, and would suggest that the homology holds reasonably up to $n_e = 5.5e/a$.

D. Properties of Mn compounds

A previous analysis⁶ of thermodynamic information on 3d-transition-metal compounds revealed that complex Mn compounds deviate from the general trend in $\Delta^0 H^{\text{st}}(T_0)$ vs n_e plots. This fact was given a qualitative explanation based on the fact that $\Delta^0 H^{\text{st}}(T_0)$ [Eq. (5)] depends on the properties of α -Mn, which is known¹³ to show an anomalously low cohesive energy in plots of E_{coh} vs n_e for the 3d transition elements. Moreover, cohesive-energy information extracted from the vibrational entropy of the Mn compounds did not deviate from the general trend,⁶ and one may ask to what extent the anomalous properties of pure Mn will be reflected in the behavior of its compounds.

The quantity E_{coh} studied here using the LMTO method shows a minimum for the MnC and MnN compounds (Figs. 4 and 5). E_{coh} depends on the properties of atomic Mn [Eq. (1)] and we find that the energies of the valence levels obtained in our calculations of the total atomic energy of Mn are exceptionally low. This is probably related to the fact that the ground-state valence configuration of the Mn atom can be described by a single-product wave function corresponding to a spherically symmetric electron density.³¹ Since our atomic calculation (like the bulk calculation) refers to an angle-averaged charge density, it is not surprising to find that it predicts the correct valence configuration for the Mn atom (cf. Table II). MnC is a metastable carbide and its properties are not known from direct measurements, but a thermodynamic analysis⁷ allowed us to get an upper limit of its cohesive energy, viz., $E_{\text{coh}} < 0.389$ Ry/atom. This implies a negative deviation from the E_{coh} values obtained for the neighboring compounds CrC and FeC. The $E_{\text{coh}}(\text{MnC})$ result in Table I, which comes from the homology approximation, leads to a dip in the E_{coh} vs n_e relation, in agreement with the LMTO calculations. The extrapolation we used to determine $E_{\text{coh}}(\text{MnN})$ is also consistent with a minimum in the cohesive energy for this compound, i.e., in line with the theoretical trend.

V. CONCLUSIONS

We have carried out a detailed study of the electronic and cohesive properties of all 3d-transition-metal carbides and nitrides in the NaCl structure, using a purely theoretical approach as well as a detailed analysis of thermodynamic information. The theoretical treatment was done with *ab initio* band-structure calculations using the LMTO method. Cohesive energies were obtained as the difference between the total energy of the compound and the total energies of its constituent atoms. The computer program for determining the total atomic energies was carefully developed and made as identical as possible to the band-structure program in order to minimize systematic errors.

In the analysis of thermodynamic information, we used direct thermochemical measurements for stable compounds, while information on metastable compounds was obtained by interpolation and extrapolation procedures. In particular, we have relied on enthalpy-of-formation values for metastable compounds derived in previous thermodynamic analyses of phase diagrams.

We find a remarkable agreement between our theoretical and our thermodynamic results, which has allowed us to analyze, not only trends, but also details in the variation of the cohesive properties of 3d metal carbides and nitrides. The fact that the theoretical cohesive energies and those obtained from thermodynamic information are separated by an almost constant shift is well known from previous calculations on the 3d metals.

MnC and MnN have relatively low cohesive energies. This is probably related to the symmetric nature of the ground-state valence configuration of the Mn atom. Another interesting case is CrN, in which the calculated E_{coh} differs significantly from what is expected from thermodynamic information. This difference may be explained, at least partly, by the fact that the theoretical cohesive energy is calculated for a paramagnetic state while CrN is known to have an antiferromagnetic ground state and a structure slightly different from the NaCl one.

The present work shows that the combination of theoretical calculations and thermodynamic analyses can be used to generate new, reliable values for properties not known from direct measurements. For instance, the information on "CoN" considered in the present work is now tested³² in a thermodynamic calculation of the Co-N phase diagram, which is not known from experiments. We expect that equally reliable results will emerge from similar work presently being carried out on other transition-metal compounds.

ACKNOWLEDGMENTS

This work has been supported by the Swedish Board for Technical Development and by the Swedish Natural Science Research Council.

- ¹K. Schwarz, *CRC Crit. Rev. Solid State Sci.* **13**, 211 (1987).
- ²V. P. Zhukov, V. A. Gubanov, O. Jepsen, N. E. Christensen, and O. K. Andersen, *J. Phys. Chem. Solids* **49**, 841 (1988).
- ³V. P. Zhukov, V. A. Gubanov, O. Jepsen, N. E. Christensen, and O. K. Andersen, *Philos. Mag. B* **58**, 139 (1988).
- ⁴V. P. Zhukov, N. I. Medvedeva, and V. A. Gubanov, *Phys. Status Solidi B* **151**, 407 (1989).
- ⁵M. Dacorogna, T. Jarlborg, A. Junod, M. Pelizzone, and M. Peter, *J. Low Temp. Phys.* **57**, 629 (1984).
- ⁶A. Fernández Guillermet and G. Grimvall, *Phys. Rev. B* **40**, 10 582 (1989).
- ⁷A. Fernández Guillermet and G. Grimvall (unpublished).
- ⁸A. Fernández Guillermet and K. Frisk, *Int. J. Thermophys.* **12**, 417 (1991).
- ⁹A. Fernández Guillermet and G. Grimvall, *Z. Metallk.* **81**, 521 (1990).
- ¹⁰O. K. Andersen, *Phys. Rev. B* **15**, 3060 (1975).
- ¹¹T. Jarlborg and G. Arbman, *J. Phys. F* **6**, 189 (1976); **7**, 1635 (1977); G. Arbman and T. Jarlborg, *Solid State Commun.* **26**, 857 (1978).
- ¹²P. Bagno, O. Jepsen, and O. Gunnarsson, *Phys. Rev. B* **40**, 1997 (1989).
- ¹³V. L. Moruzzi, J. F. Janak, and A. R. Williams, *Calculated Electronic Properties of Metals* (Pergamon, New York, 1978).
- ¹⁴A complete set of density-of-states and band curves is found in J. Häglund, Trita-tfy-90-05, The Royal Institute of Technology, Stockholm, Sweden, 1990.
- ¹⁵Scientific Group Thermodata Europe (SGTE) Data for Pure Elements, compiled by A. T. Dinsdale, NPL Report No. DMA(A) 195 (National Physical Lab., Teddington, UK, 1989) (unpublished).
- ¹⁶JANAF Thermochemical Tables, 3rd ed., edited by M. W. Chase, C. A. Davies, J. R. Downey, Jr., D. J. Frurip, R. A. McDonald, and A. N. Syverud [*J. Phys. Chem. Ref. Data* **14**, Suppl. 1 (1985)].
- ¹⁷P. D. Desai, *Int. J. Thermophys.* **7**, 213 (1986).
- ¹⁸P. D. Desai, *J. Phys. Chem. Ref. Data* **16**, 91 (1987).
- ¹⁹D. Garvin, *Bull. Alloy. Phase Diagrams* **2**, 262 (1981).
- ²⁰L. Brewer, "The Cohesive Energy of the Elements", Report LBL-3720 Ref., Lawrence Berkeley Laboratory, University of California, 1977.
- ²¹K. A. Gschneidner, in *Scandium*, edited by C. T. Horowitz (Academic, London, 1975), pp. 152-251.
- ²²O. Kubaschewski and C. B. Alcock, *Metallurgical Thermochimistry*, 5th ed. (Pergamon, Oxford, 1979).
- ²³P. Roedhammer, W. Weber, E. Gmelin, and K. H. Rieder, *J. Chem. Phys.* **64**, 581 (1976).
- ²⁴Value quoted in V. P. Zhukov, V. A. Gubanov, and T. Jarlborg, *J. Phys. Chem. Solids* **46**, 1111 (1985).
- ²⁵L. E. Toth, *Transition Metal Carbides and Nitrides* (Academic, New York, 1971).
- ²⁶G. Grimvall and J. Rosén, *Int. J. Thermophys.* **4**, 139 (1983).
- ²⁷M. Hillert and L-I. Staffansson, *Acta Chem. Scand.* **24**, 3618 (1970).
- ²⁸A. Fernández Guillermet and K. Frisk (unpublished).
- ²⁹L. Brewer and O. Krikorian, *J. Electrochem. Soc.* **103**, 38 (1956).
- ³⁰L. M. Corliss, N. Elliott, and J. M. Hastings, *Phys. Rev.* **117**, 929 (1960).
- ³¹V. L. Moruzzi, A. R. Williams, and J. F. Janak, *Phys. Rev. B* **15**, 2854 (1977).
- ³²A. Fernández Guillermet and S. Jonsson (unpublished).
- ³³P. V. Villars and L. D. Calvert, *Pearson's Handbook of Crystallographic Data for Intermetallic Phases* (American Society for Metals, Metals Park, OH, 1985).
- ³⁴F. Lihl, P. Ettmayer, and A. Kutzelnigg, *Z. Metallk.* **53**, 715 (1962).
- ³⁵Z. Nishiyama and R. Iwanaga, *Mem. Inst. Sci. Ind. Res. Osaka Univ.* **9**, 74 (1952).
- ³⁶O. Schmitz-Dumont and N. Kron, *Angew. Chem.* **67**, 231 (1955).
- ³⁷T. B. Joyner and F. H. Verhoek, *J. Amer. Chem. Soc.* **83**, 1069 (1961).